HardwareX 22 (2025) e00654

Contents lists available at ScienceDirect

HardwareX

journal homepage: www.elsevier.com/locate/ohx

Hardware Article

A portable soil surface roughness instrument for automatic two-dimensional profile roughness measurement in the field

Gang Sun [a,*], Xiu Wang [b], Shuai Gao [a], Jinmei Pan [a], Qinhuo Liu [a], Wenjiang Huang [a]

[a] State Key Laboratory of Remote Sensing Science, Aerospace Information Research Institute, Chinese Academy of Sciences, Beijing 100101, China
[b] Intelligent Equipment Research Center, Beijing Academy of Agriculture and Forestry Sciences, Beijing 100097, China

ARTICLE INFO

Keywords:
Soil surface roughness
Relevant length
Instrument
Radar remote sensing
Laser rangefinder
Pin meter

ABSTRACT

Soil surface roughness, characterized by the unevenness of the soil surface, is a critical parameter influencing radar backscatter coefficients and microwave emissivity, and is essential for applications in agriculture, soil science, climate modeling, and geology. Current roughness measurement methods, such as manual pin meters and photogrammetry, face limitations in field portability, automation, and cost efficiency. To overcome these challenges, this study introduces a novel, portable instrument utilizing automated two-dimensional rotary laser scanning to quantify surface roughness. The device's innovative design integrates a tripod-mounted laser scanner that generates 1 cm-resolution horizontal profiles by calculating surface heights from rotation angles and distances, eliminating manual intervention and enabling rapid field deployment. Compared to traditional contact methods or LiDAR systems, the instrument achieves comparable accuracy (R2 = 0.97 vs. pin meters) while offering significant advantages in portability (<5 kg total weight), automation (full-profile measurement in < 30 s), and affordability (estimated cost <$2,705). Field experiments validated its ability to compute roughness parameters (RMS height, correlation length) critical for microwave remote sensing and soil erosion modeling. By bridging the gap between laboratory-grade precision and field practicality, this instrument provides researchers and agronomists with a cost-effective tool to advance microwave remote sensing, precision agriculture, climate forecasting, and soil conservation efforts.

Specifications table

Hardware name	*A portable soil surface roughness instrument for automatic two-dimensional profile roughness measurement in the field*
Subject area	• Environmental, planetary and agricultural sciences • Educational tools and open source alternatives to existing infrastructure
Hardware type	• Measuring physical properties and in-lab sensors • Field measurements and sensors • Electrical engineering and computer science
Closest commercial analog	Lidar scanner, Pin meter
Open source license	GPL General Public License v3.0
Cost of hardware	Approximately *$USD2,705*
Source file repository	https://doi.org/10.17632/x8dbztc9fs.1

* Corresponding author.
E-mail address: sungang@aircas.ac.cn (G. Sun).

https://doi.org/10.1016/j.ohx.2025.e00654
Received 25 December 2022; Received in revised form 13 April 2025; Accepted 17 April 2025
Available online 19 April 2025
2468-0672/© 2025 Published by Elsevier Ltd. This is an open access article under the CC BY-NC-ND license (http://creativecommons.org/licenses/by-nc-nd/4.0/).

1. Hardware in context

Soil surface roughness, defined as the unevenness of the surface caused by soil texture, aggregates, rock fragments, and land management practices, plays a critical role in influencing the radar backscattering coefficient and microwave emissivity of the surface (rougher soil has a higher emissivity and reduced sensitivity to soil moisture compared to smooth soil with otherwise identical characteristics) [1]. Soil surface roughness has important applications in agriculture, soil science, weather and climate prediction, geology, and other fields. In agriculture and soil science, roughness affects infiltration, flood, and soil erosion and some predictive models has been developed [2]. In the field of climate and weather prediction, soil storage and evaporation also depend on surface roughness [3]. In geology, the geological element information of wind-eroded sandstone can be determined based on surface roughness [4,5]. Surface roughness can be divided into two types: geometric roughness and aerodynamic roughness. Geometric roughness is often used in remote sensing, particularly in microwave remote sensing. Surface parameterization is essential for developing practical soil moisture inversion models. However, the acquisition of soil roughness is a limiting factor and developing simple correction methods is difficult [6]. Research has shown that the influence of soil surface roughness on the backscatter coefficient is generally equal to or greater than that of soil moisture [7]. Therefore, in the development of microwave remote sensing inversion of surface parameters, surface roughness is a focus of research. To correct the influence of roughness on the backscattering coefficient with measured data, the most common method is to collect soil roughness synchronously in observation tests [8]. Only by resolving this challenge can we establish a correct surface microwave scattering model and effectively carry out parameter inversion.

At present, in the field of remote sensing, RMS (root mean square) height and correlation length based on single scale are used to describe vertical and horizontal surface roughness [9]. These two parameters are not fixed and depend on the length of the measurement section and the resolution of the measurement division [10]. The RMS height h_{rms} is a measure of the standard deviation of surface heights. It is calculated as:

$$h_{rms} = \sqrt{\frac{1}{N}\sum_{i=1}^{N}(z_i - \overline{z})^2} \tag{1}$$

Where:
N is the total number of data points,
z_i is the height(mm) at the $i-th$ point,
$\overline{z}$ is the mean height(mm), calculated as:

$$\overline{z} = \frac{1}{N}\sum_{i=1}^{N} z_i \tag{2}$$

The correlation length l describes the distance over which surface heights are correlated. It is derived from the autocorrelation function $C(\tau)$:

$$C(\tau) = \frac{\sum_{i=1}^{N-\tau}(z_i - \overline{z})(z_{i+\tau} - \overline{z})}{\sum_{i=1}^{N}(z_i - \overline{z})^2} \tag{3}$$

The correlation length l is the lag distance τ at which the autocorrelation function decays to $1/e$ (approximately 0.368):

$$C(l) = \frac{1}{e} \tag{4}$$

Where:
z_i is the height (mm) at the $i-th$ point,
$\overline{z}$: is the mean height (mm),



Fig. 1. Roller chain [24].

τ: is lag distance (cm),

l: Correlation length (cm), the distance at which $C(\tau)$ decays to $1/e$.

There are two main categories of measurement methods for surface roughness: contact and non-contact. The Contact method refers to the use of a panel or pin roughness meter or chains to measure soil surface roughness. The pin meter method is one of the earliest technologies used for quantitative research of soil surface roughness [1]. As seen in Fig. 1, it consists of a row of pins arranged vertically over the soil surface coupled to a camera to record the images of the pins and obtain the profile. When measuring, the pins contact the ground and the surface relief profile is drawn by recording the position of the pin tail [11]. The panel meter method is to insert a panel with a grid drawn into the soil and draw the profile by recording the position of the soil surface on the grid [12]. Roughness plate measuring technology is cheap and convenient to use, and it is still the observation method used in many studies. Although the plate is cheaper and more convenient, it needs to be inserted into the soil, which is difficult to use when the ground is relatively hard, and there is also greater uncertainty in the process of photographing and digitizing the profile, which can limit its usefulness. As shown in Fig. 2, the chain method is based on the principle that as a chain of a given length, L1, is placed across a surface, the horizontal distance covered L2, will decrease as the roughness increases [13]. The biggest limitation of contact measurement technology is that it can interfere with the observation object, particularly the observation error of microtopography caused by the destruction of loose particles or soft wet ground surface cannot be ignored [14]. Additionally, due to the portability of the equipment, the sampling length is relatively limited. For the pin meter, due to the size of the pin tail, the sampling interval can only reach 1 ~ 2.5 cm.

Non-contact methods include structured light laser scanning [14], laser ranging [5,11] or ultrasonic [1] scanning, lidar measurement [1,12], close-range photogrammetry [16,17,18], SfM(Structure from Motion) photogrammetry [2,9,19,20], etc. Structured light three-dimensional (3D) scanning technology is introduced into the field of surface parameter measurement. When measuring, the grating projection device projects a specific coded structured light onto the surface of the object to be measured, the camera synchronously captures the corresponding image, then decodes and calculates the phase of the image, and uses matching technology and triangle measurement principle to calculate the 3D coordinates of feature pixel points. Finally, the measurement data is processed to automatically generate roughness parameters. The biggest disadvantage of the structured light method is that it is difficult to apply it directly in the field because of the large impact of ambient light. Compared with contact measurement technology, non-contact measurement technology based on laser scanning was introduced into surface observation relatively late. As show in Fig. 3, a laser profiler consists of five parts: laser emission source, reflective focusing device, reflective sensing device, processing electronic components, and a guide rail. The light source emits a laser vertically to the ground, and the reflected light projects onto the detector through the focusing device. As the instrument moves on the guide rail, the focusing position of the reflected light varies with the fluctuation of the ground height. The electronic components process the signal of the detector, record the position of the peak intensity, and then obtain the ground height profile [11,15].The roughness-related parameters used in current applications are all defined based on two-dimensional elevation profile. This is because, in the past, acquiring elevation information across the entire surface required the use of large frame structures to support profile measurements at multiple locations—a process that was not only costly but also time-consuming and labor-intensive. Photogrammetry is another common non-contact measurement technology. This technology obtains a digital elevation model (DEM) by taking stereo image pairs with 2 cameras [17,18,22]. The multi-view photogrammetry method is also employed to analyze soil surface roughness [19]. Photographs are captured centripetally from multiple positions around



Fig. 2. Pin meter [25].



Fig. 3. Laser profiler [21].

the analyzed surface. Following image processing using photogrammetric software to generate a point cloud, a digital elevation model is derived, and roughness parameters are subsequently calculated. A low-cost, portable and robust optical equipment through an illumination system with a line laser and monocular vision has been proven to be valid [14]. In terms of costs and ease of use in the field, a depth-sensing technique originating in the gaming industry [23] has recently become promising for soil sciences: the Xtion Pro method [5]. Compared with the profile data, DEM carries more abundant information and can better describe surface characteristics. Moreover, based on DEM data, arbitrary surface roughness parameters can be calculated theoretically.

It can be concluded that each measurement technique has its specific field of application, determined by factors such as required accuracy, resolution, field mobility, and available budget [9]. In general, contact methods, such as the roller chain and pin meter, are limited in their applicability due to their restricted resolution and precision, as well as their labor-intensive and impractical nature in field conditions [5]. This study addresses two critical limitations in current measurement systems through three core innovations: 1) Portable and real-time parameter acquisition: The proposed embedded processing architecture eliminates computational post-processing stages (15–30 min/dataset in conventional LiDAR systems and photogrammetric devices) by integrating 32 bits MCU, enabling on-site output of end-user parameters within 30 seconds. 2) Robust operation under suboptimal lighting conditions: Where existing solutions (photogrammetry) mandate high and stable ambient illumination for reliable operation. The laser ranging sensor used in this instrument can work stably in complex light environments. This study aims to provide an open-source, low-cost, portable, and robust instrument to characterize the two-dimensional (2D) profile roughness. A set of core features are presented. Additional customization will be required, depending on the application.

2. Hardware description

In the prior art scheme in Fig. 3, the frame scanning structure is complex, and the weight is difficult to reduce. This paper proposes a single-point rotary scanning scheme based on the principle of rotary scanning. The schematic diagram of the scheme is shown in Fig. 4. The most notable distinction between this instrument and traditional laser measuring devices mounted on one-dimensional or two-dimensional motion platforms is the use of rotational movement instead of translational movement. This innovation eliminates the need for complex and costly motion platforms, significantly enhancing portability and reducing overall costs.

The operational procedure is as follows: First, the instrument is positioned on the surface to be measured, and the laser ranging sensor is adjusted vertically downward. The reference height h_0 is measured. Based on h_0, the rotation angle a_i required to offset one measurement interval x in the horizontal direction is calculated. The laser ranging sensor can rotate left and right under the drive of the rotating mechanism. After the laser ranging sensor rotates to the specified angle, it projects a laser to measure the distance and obtain the tilt length l_i According to the angle b_i between the current laser and the vertical direction, the actual ground height hi of the point can be obtained by trigonometry. The instrument performs 50 scans to the left to measure height data for a 50 cm section of the ground on the left side. It then performs 50 scans to the right to measure height data for a 50 cm section on the right side. Finally, the surface roughness parameters for the total measured length of 1 m are automatically calculated. This approach ensures efficient and accurate data collection while maintaining simplicity and cost-effectiveness.

As illustrated in Fig. 5, the proposed soil surface roughness instrument comprises 7 key components: 1) a microcontroller unit, 2) a laser rangefinder, 3) a servomotor, 4) a power unit, 5) a tripod, 6) a communication module, and 7) a smartphone.

The microcontroller unit is an Arduino-compliant module. Arduino is commonly used for various DIY projects because of its low cost and versatility connecting nearly unlimited sensors through extended general-purpose input/output modules. The core of the microcontroller unit is an ESP32-WROOM-32 module (Espressif Systems, Shanghai, China) equipped with powerful Wi-Fi + Bluetooth LE modules that target a wide variety of Internet-of-Things (IoT) applications. The develop software, Arduino IDE 2, features a board

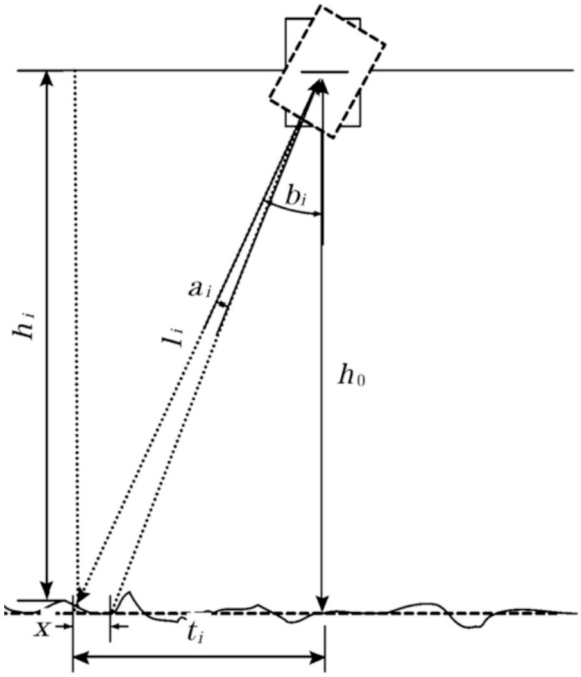


Fig. 4. Schematic diagram of instrument measurement.

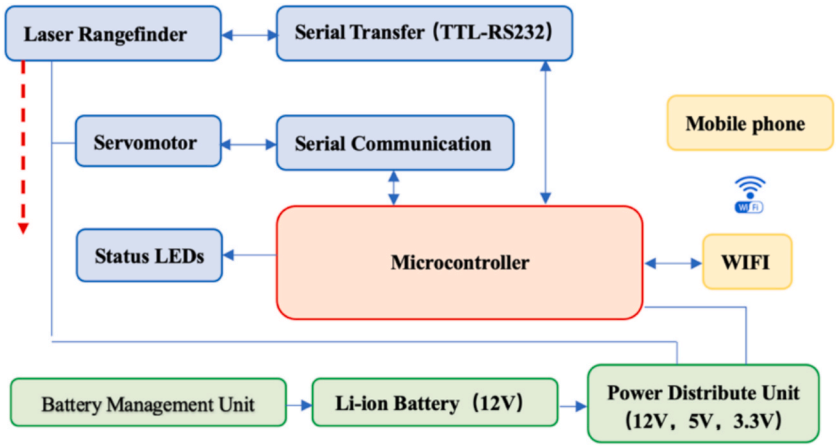


Fig. 5. Hardware schematic.

manager tool that is used to install specific ESP32 core on your local computer. Arduino's simple development method enables developers to pay more attention to creativity and implementation, complete their own project development faster, greatly save on the cost of learning, and shorten the development cycle.

A compact servomotor (MG4005-I10 V2, LK-TECH, Shanghai, China) is used to rotate the laser rangefinder. It adopts the integrated design of the motor and planetary reducer, integrates high-precision absolute value encoder, and cooperates with a double closed-loop control algorithm to greatly improve the accuracy of torque, position, and speed feedback. The servomotor works in incremental position closed-loop mode with a minimum resolution of 0.01 degrees and a rated torque of 1Nm. The servomotor communicates with the microcontroller through a Universal Asynchronous Receiver/Transmitter (UART) serial port.

A highly accurate laser rangefinder (DEN-10-500, Dimetix AG, Switzerland) was chosen to measure the distance. It can measure distances of up to 500 m, with an accuracy of $\pm$ 1 mm. Because of its high measurement rate of up to 50 Hz, it is suitable for high-speed applications. Various communication interfaces are integrated inside the sensor. RS-232 interface is used to connect the sensor and the microcontroller. A TTL-RS232 convert module is adopted to realize the level conversion.

The instrument is powered by a rechargeable 3S lithium polymer (LiPo) battery which provides a nominal output voltage of 12 V. The output voltage varies from 12.6 V when fully charged, down to 9.6 V, when the internal battery regulator disables the battery from over-discharge. The most significant power source needed for this instrument is for the rotation of the servomotor. This LiPo battery

has a high charge/discharge rate and can provide power for the most demanding electric servomotor. The power requirement for the microcontroller is relatively minimal, so a voltage regulator connected to the battery was used to provide 2 A with 5 V DC power. To optimize power usage, the device incorporates a low-power sleep mode that activates during idle periods between measurements. In field tests, the device demonstrated consistent performance over multiple days of operation, with daily usage averaging 8–10 h. Recharging the battery to full capacity takes approximately 1–2 h using the provided 5 V/1A USB charger. For extended field campaigns, users are advised to carry a portable power bank to ensure uninterrupted operation.

This instrument potentially provides real-time data access to the WLAN network or can be set up to provide its hotspot in case of unavailable WLAN. It can be considered an important feature that no existing WLAN is necessary. If the instrument is used as an access point, it provides the WLAN for the connection terminal smartphone and any monitoring device with a browser (laptop, tablet, etc.).

The features of the presented soil surface roughness instrument could be summarized as follows:

- The instrument can instantly get the roughness and the correlation length results without further data processing.
- The maximum profile length can be 1 m and the sample interval is 1 cm.
- The instrument can operate in the temperature range of 0-50°C.
- The measurement time is less than 30 s.
- The compact size of the instrument and its low weight make it easier to carry and set up.
- The instrument can be connected by smartphone or computer to the built-in Wi-Fi hotspot. It provides a browser-accessible user interface for easy data retrieval.
- The Measuring accuracy of the rangefinder is up to ± 1.0 mm (@ 2σ)

3. Design files summary

The design files consist of all the files needed to make and run the soil surface roughness instrument. Table 1 shows the list of design files.

- The Rangefinder adapter is the connection part for the instrument box and rangefinder.
- The 2D_CAD_rangefinder_DEN-10–500 and 2D_CAD_servomotor_MG4005-I10-V2 are the CAD files of two part.
- The hardware schematic presents the electronic schematic of the instrument, the main components, and their connections.
- The roughness_firmware_20220829 there is an Arduino source code of the instrument. The code can be changed for customization.
- Video_Instrument_application720p presents the application of the instrument in the field.

4. Bill of materials summary

Table 2 shows the components that are needed to reproduce the board.

Table 1
Design files.

Design file name	File type	Open source license	Location of the file
Rangefinder_adapter	stl	GPL 3	https://doi.org/10.17632/x8dbztc9fs.1
2D_CAD_rangefinder_DEN-10-500	pdf	CC BY-SA	https://doi.org/10.17632/x8dbztc9fs.1
2D_CAD_servomotor_MG4005-I10-V2	jpg	CC BY-SA	https://doi.org/10.17632/x8dbztc9fs.1
hardware_schematic	png	GPL 3	https://doi.org/10.17632/x8dbztc9fs.1
roughness_firmware_20220829	ino	GPL 3	https://doi.org/10.17632/x8dbztc9fs.1
Video_Instrument_application720p	mp4	GPL 3	https://doi.org/10.17632/x8dbztc9fs.1

Table 2
Bill of materials.

Designator	Component	Number	Cost per unit —USD	Total cost — USD	Source of materials	Material type
ESP-WROOM	ESP32-WROOM-32 microcontroller module	1	$4	$4	AliExpress-ESP32 Development Board	Electronics
DC converter	Voltage regulator (or similar)	1	$3	$3	https://www.amazon.com	Electronics
LiPo battery	3S 12 V LiPo battery with DC charger	1	$6	$6	https://www.amazon.com	Electronics
Servomotor	MG4005-I10 V2 motor with planetary reducer	1	$140	$140	https://s.vnshu.com/3GR2tx	Electronics
Rangefinder	DEN-10-500 distance sensor	1	$2500	$2500	https://dimetix.com/	Electronics
Button	12 mm push button switch	1	$0.5	$0.5	https://www.amazon.com	Electronics
Level bubble	Mini liquid bubble	1	$0.5	$0.5	https://www.amazon.com	Other
Power plug	12 mm DC power male plug	1	$0.5	$0.5	https://www.amazon.com	Electronics
Plastic box	Waterproof IP65 ABS plastic box	1	$0.5	$0.5	AliExpress-ABS box, 100*68*50	Other
Tripod	Tripod with fluid head	1	$50	$50	AliExpress-Tripod Yunteng	Other

a) Cover the box with the upper lid and glue it securely in place.
b) The final assembled instrument is shown in Fig. 7.

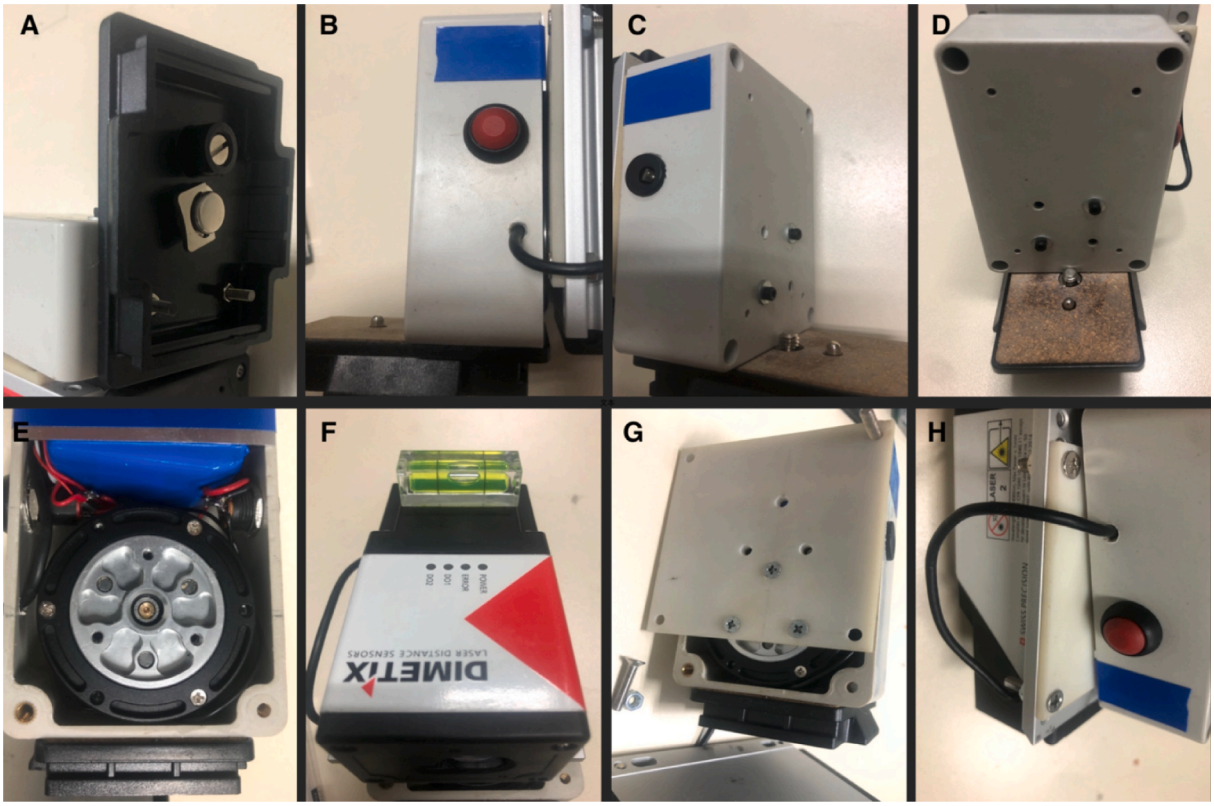


Fig. 6. Build instructions for steps 2 to 10. A) Prepare the quick-release plate. B) Install push button. C) Install power plug. D) Mount the servomotor. E) Mount the servomotor, In the other direction. F) Attach the level bubble. G) Install electronic components and battery. H) Final assembly.

5. Build instructions

The following steps provide a step-by-step guide for building and assembling the soil surface roughness instrument. Please see Fig. 6 for a diagram of the assembly.

5.1. Assembling the physical support

1. **Remove the upper cover** of the waterproof and dustproof IP65 ABS plastic box. All subsequent steps are performed on the main body of the box.
2. **Prepare the quick-release plate** (Fig. 6A):
   a) Detach the quick-release plate from the tripod.
   b) Create two 3 mm circular holes on the plate.
   c) Make two corresponding 3 mm circular holes on the left side of the box, ensuring a 30 mm distance between them.
   d) Insert two 2 mm bolts through the holes with the threads facing outward.
   e) Secure the box and quick-release plate using nuts on each side.
3. **Install the push button** (Fig. 6B):
   a) Create a 12 mm circular hole on the right side of the box.
   b) Insert the push button and secure it with a nut.
   c) Ensure the center of the hole is 60 mm from the bottom side of the box.
4. **Install the power plug (**Fig. 6C):
   a) Create a 12 mm circular hole on the left side of the box.
   b) Insert the power plug and secure it with a nut.
   c) Ensure the center of the hole is 60 mm from the left side of the box.
5. **Mount the servomotor**: (Fig. 6D&E)
   a) Create four 3 mm circular holes at the vertices of a square on the front side of the box.



Fig. 7. View of the assembled instrument.

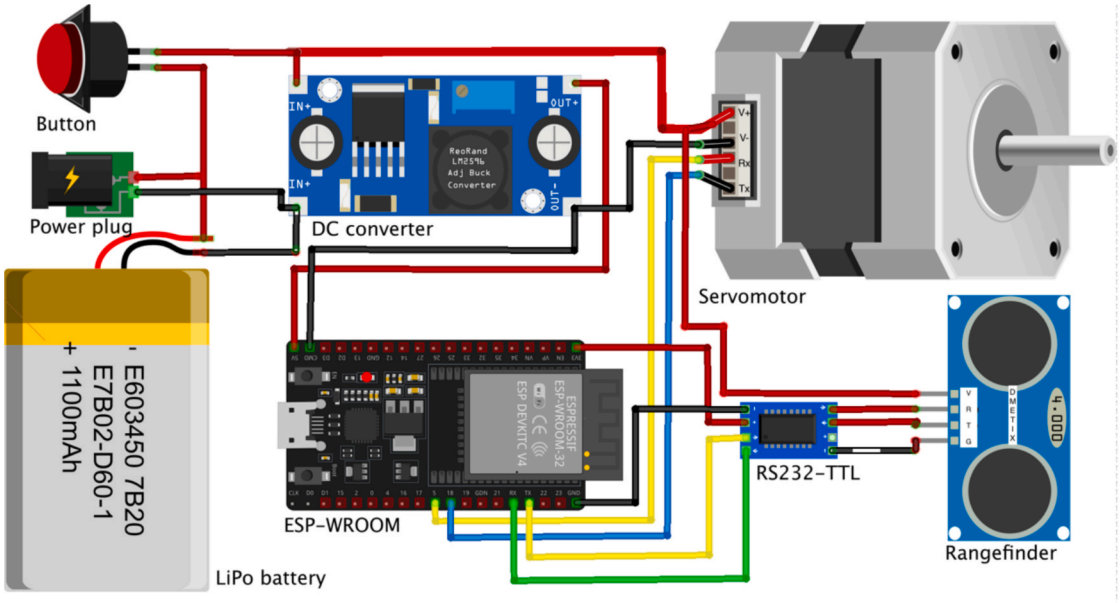


Fig. 8. Connection diagram of the hardware of the instrument.

b) Insert four 2.5 mm bolts through the holes with the threads facing inward.
c) Fix the servomotor onto the box using these bolts.

6. **Attach the level bubble** (Fig. 6F):
   a) Glue the level bubble onto the rangefinder.
7. **Prepare the connection plate (Rangefinder adapter)** (Fig. 6G):
   a) 3D print the connection plate using Polylactic acid (PLA) or Acrylonitrile butadiene styrene (ABS).
   b) Insert four 2.5 mm bolts through the plate with the threads facing the servomotor, and secure the plate to the servomotor.
   c) On the opposite side of the plate, insert four 3 mm bolts with the threads facing the rangefinder, and secure the plate to the rangefinder.
8. **Drill a cable entry hole** (Fig. 6H):
   a) Drill a 3 mm hole on the right side of the box.

b) Insert the rangefinder cable into the box through this hole.

9. **Install electronic components and battery** (Fig. 6H):
   a) Place the electronic components and battery inside the box.
10. **Final assembly**:
   a) Cover the box with the upper lid and glue it securely in place.
   b) The final assembled instrument is shown in Fig. 7.

5.2. Assembling the electronic circuit

Fig. 8 shows the scheme of the proposed device, where the elements and connections are described. All the parts are very common and can be bought online or from electronics and hardware retailers. Follow the step-by-step procedure to rebuild the system.

1. Assemble the power system: Solder the cables from the LiPo battery and the power plug to the DC converter. Connect a power button in series in the positive pole of the circuit. This button works as the main switch of the instrument. Solder the output cable of the DC converter (OUT +, OUT-) to the ESP-WROOM in the 5 V and GND position according to the corresponding polarity. Pay attention to the polarity.
2. Assemble the servomotor: The power of the servomotor is fed by a 12 V battery. Join the power cable coming out for the servomotor with appropriate wires and connect it to the DC converter in the IN + and IN- positions. Wire PIN 5 and PIN 18 to the Tx and Rx of the servomotor by soldering using the appropriate wires.
3. Assemble the rangefinder: The rangefinder is powered by 12 V battery, so join the power cable coming out for the rangefinder with appropriate wires and connect it to DC converter in the IN + and IN- positions. ESP-WROOM delivers 3.3 V power to the RS232-TTL module with the PIN 3 V3 and pin GND connected with its + and – positions. The serial port pins Tx and Rx from ESP-WROOM are soldered to RS232-TTL by −> and <- terminals. Then at the output side of the RS232-TTL, the −> and <- terminals are joined by wires with the R and T terminals of the rangefinder. In this way, the TTL signal is transferred to the RS232 signal and the communication between the microcontroller and the distance sensor is established.
4. Optionally, the RS232-TTL module and DC converter can be attached directly to the ESP-WROOM. To do so, contact pins are used to solder them with the corresponding pins.

5.3. Installing the firmware

1. Plug the ESP32 board into your computer through a USB cable. With your Arduino IDE open, follow these steps:
2. Select your Board in Tools > Board menu (In this case it's the ESP32 Dev Module):
3. Select the virtual serial port of the board (If the COM Port in your Arduino IDE does not exist, the CP210x USB to UART Bridge VCP Drivers should be installed).
4. Open the firmware of the instrument (roughness_firmware_20220829), and a new sketch will be opened in the Arduino IDE.
5. Press the Upload button in the Arduino IDE. Wait a few seconds while the code compiles and uploads to your board (If ESP32 is not in flashing/uploading mode, hold-down the BOOT button in your ESP32 board).
6. Press the ESP32 on-board Enable button and the firmware will work.

5.4. Potential safety concerns

The instrument emits a visible laser beam, which emerges from the front of the instrument. The laser is a CLASS 2 laser product under IEC/EN 60825–1:2014. It may be hazardous to the eyes, so DO NOT look directly at the laser beam or aim it at other people unnecessarily.

6. Operation instructions

6.1. Setup and adjust the instrument

Mount the instrument onto the tripod. The instrument is equipped with a quick-release plate, which can be directly installed on the tripod. First, turn the locking clip of the quick-release plate outward, and the button below the quick-release plate will pop up. Then, insert the quick-release plate of the instrument host, press down the button on the quick-release plate, and the locking clip will spring back automatically to lock the instrument.

Tilt the instrument about 10 degrees. First, loosen the "tilt and pitch adjusting screws", adjust the angle by pushing the "handle" up and down, tilt the host about 10 degrees, and then tighten the "tilt and pitch adjusting screws". The purpose of the adjustment is to make the laser emitted by the instrument tilt outward to prevent the laser emitted by the sensor from hitting the tripod. The adjusted angle is shown in Fig. 9a below.

Adjust the height of the tripod legs and lift the center axis by turning the "crank" on the tripod. To reduce measurement error, the instrument should be erected as high as possible. The adjusted instrument should look as shown in Fig. 9b.

Power on the instrument. Press the switch button on left side of the instrument to power it on.

Connect the smartphone to the instrument by Wi-Fi.

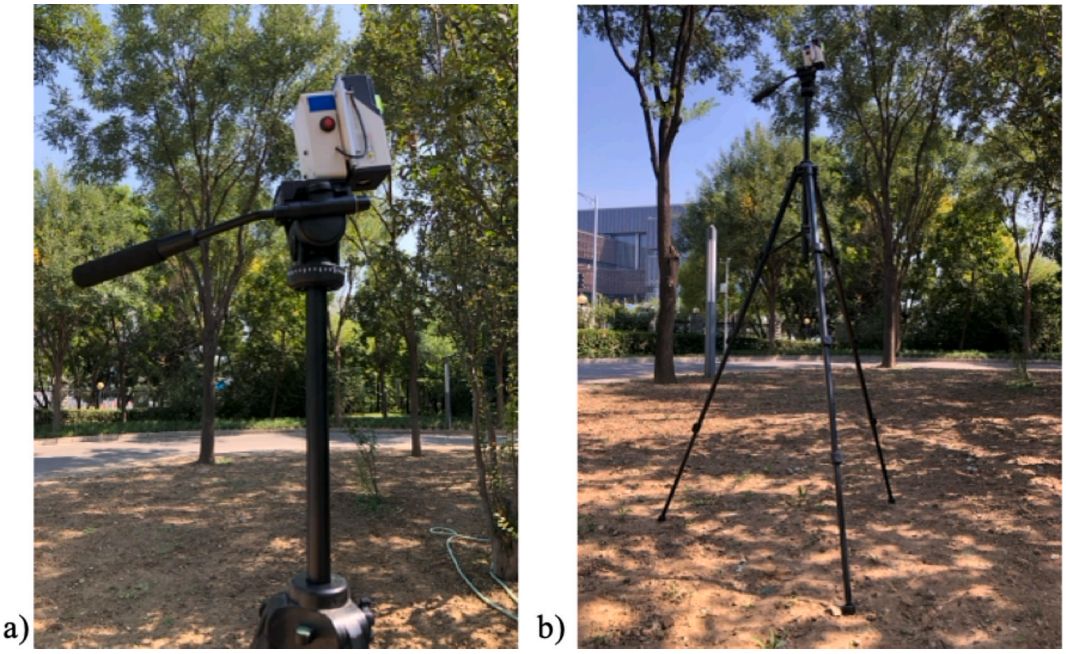


Fig. 9. Tilt the instrument. a) Adjusting the angle of the instrument. b) The adjusted instrument photo.

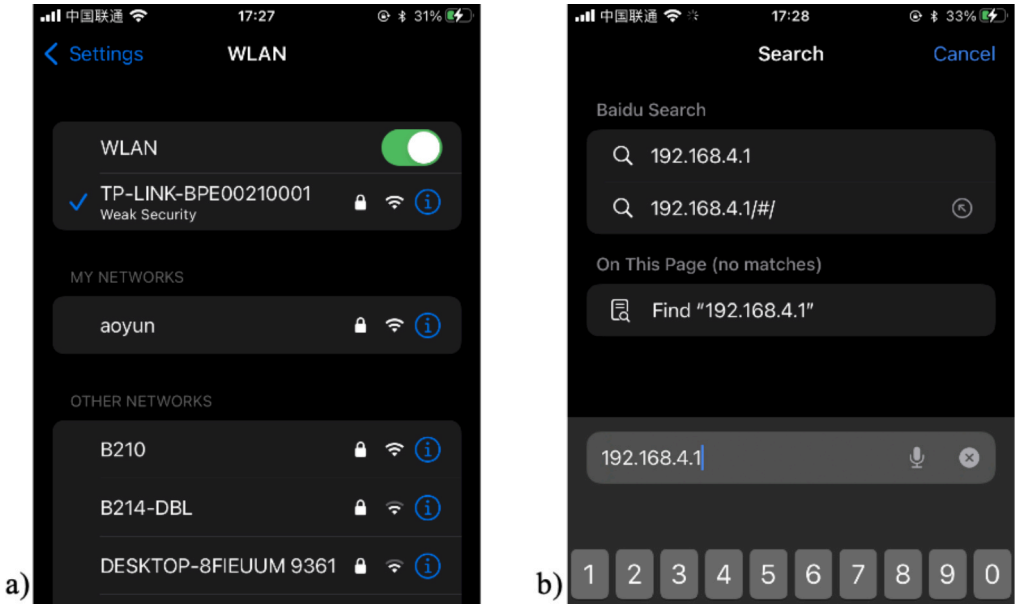


Fig. 10. Connect the instrument. a) WLAN Setting part. b) Entering the address of the instrument.

- From your Home screen, go to Settings > Wi-Fi.
- Turn on Wi-Fi. Your smartphone will automatically search for available Wi-Fi networks.
- Tap the Wi-Fi network named TP-LINK −BPE0021001 to join. You may be asked to enter the network's password or agree to terms and conditions before you can connect. The initial password is 12345678.
- Open the browser on your smartphone and enter the web address 102.168.4.1. Press Go to access the server on the instrument host. The operation interface of the browser is as shown in Fig. 10.
  Adjust the three legs of the tripod to center the bubbles on the host. You can also drag the "Adjust vertical" button, as shown in Fig. 11a on the smartphone, to adjust the angle of the instrument to center the horizontal bubble, as shown in Fig. 11b.

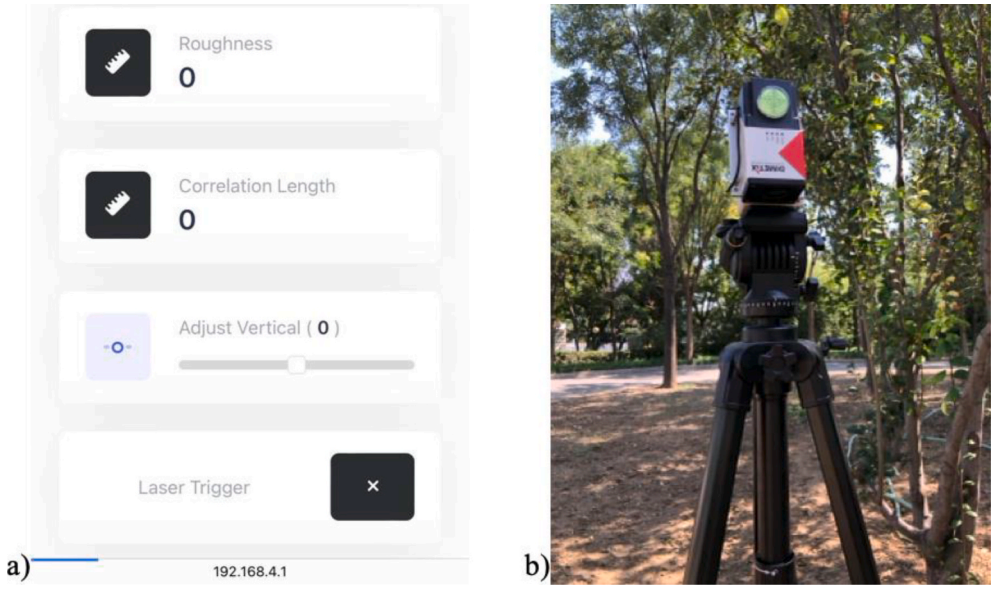


Fig. 11. Adjust the level of the instrument. a) The user interface of the instrument. b) Instrument adjustment photo.

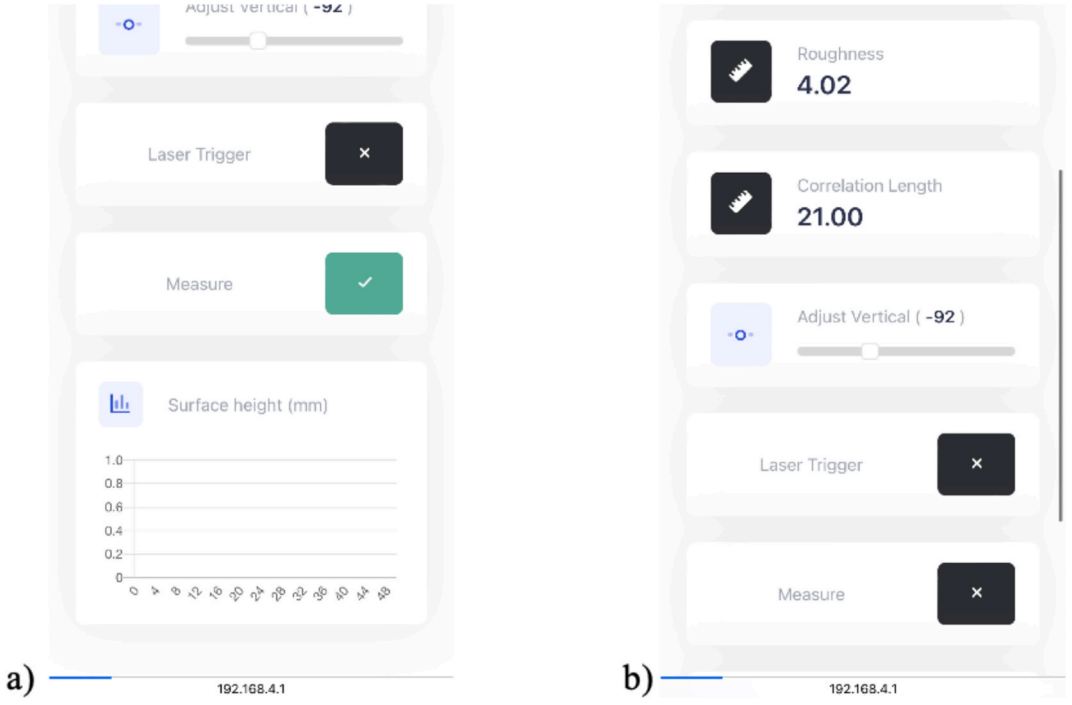


Fig. 12. The interface of the measurement. a) The lower section of the user interface. b) The upper section of the user interface.

6.2. *Measurement*

As illustrated in Fig. 12a, click the "Measure" button to initiate the surface roughness measurement. This action will activate the laser; **please avoid direct exposure to the laser beam**. Once the measurement is complete, the results will be displayed at the top of the web page, as shown in Fig. 12b. The roughness values are reported in millimeters (mm), while the correlation length is provided in centimeters (cm).

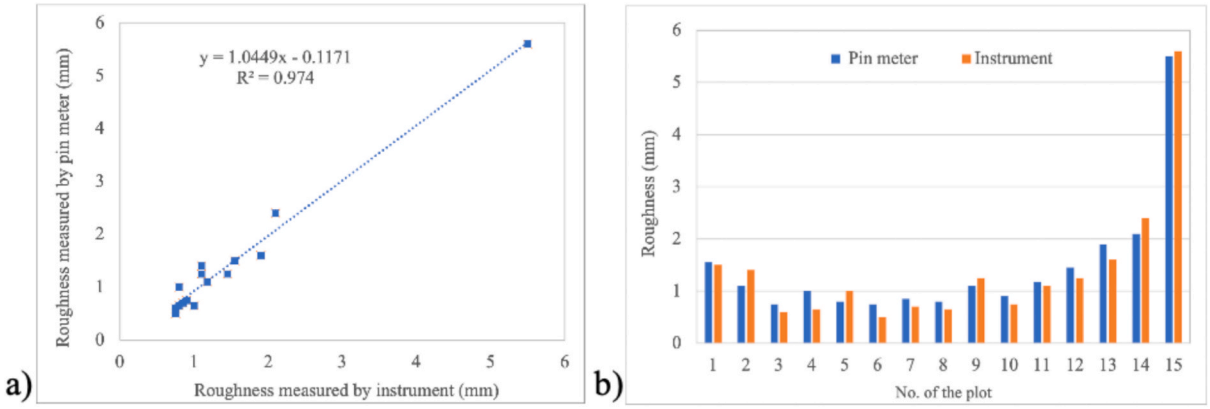


Fig. 13. Comparison of roughness tested by pin meter and the instrument. a) Linear regression comparison of roughness measurements (R^2 = 0.974). b) Comparison of roughness measurements across sample points.

7. Validation and characterization

7.1. Validation

To validate the performance of the proposed instrument, a field test was conducted in Otog Banner, Inner Mongolia, in September 2022. The experimental site was selected based on terrain relief and vegetation coverage conditions, featuring scattered rocks that enhance topographic variability. It exhibits significantly lower vegetation coverage due to salinization, desertification, and adverse moisture conditions, with hard-textured substrates ensuring stability for repeated trials. The combination of degradation factors (salt accumulation, sand mobility, and drought stress) and natural geomorphic complexity allows controlled simulations of ecological dynamics while maintaining experimental reproducibility. The test was performed on two distinct soil types: silty loam and sandy loam. For comparison, roughness measurements were obtained using a pin meter as a reference method. Fifteen measurement points were selected, and surface roughness parameters were calculated using both the proposed instrument and the pin meter.

The validation procedure involved two steps. First, the proposed instrument was used to measure the roughness parameters at each point. Subsequently, the pin meter was employed to measure the same soil surface sections at the corresponding locations. The pin meter method required on-site photography, followed by post-processing using specialized software to extract the surface profile and calculate roughness and correlation length parameters.

The results of the roughness parameters measured by both instruments are presented in Fig. 12. Linear regression analysis was performed on two comparative datasets, yielding a first-order equation ($y = 1.0449x - 0.1171$) with coefficients derived through least squares estimation. The coefficient of determination ($R2 = 0.974$) was calculated to evaluate model fit, indicating that 97 % of the variance in the dependent variable is explained by the linear relationship. A strong correlation was observed between the roughness values obtained from the proposed instrument and those derived from the pin meter (Fig. 13a), with a maximum error not exceeding 0.8 cm (Fig. 13b). The close agreement between the two methods confirms the accuracy and reliability of the proposed instrument for measuring surface geometric roughness, meeting the requirements for field applications.

7.2. Summary and future work

In this study, we developed an open-source, portable instrument designed for rapid and accurate measurement of soil surface roughness in field conditions. The device integrates a high-precision laser rangefinder, a compact servo motor equipped with a planetary reducer, and wireless communication capabilities to ensure reliable and efficient data collection in outdoor environments. The proposed instrument demonstrates high accuracy, with roughness measurements showing strong correlation to pin meter results and a maximum error of less than 0.8 cm, confirming its reliability for field-based surface roughness measurements. At this current resolution, the instrument is limited to characterizing roughness at the scale of nugget size, medium-sized soil aggregates, and larger fractional components. It is unable to capture micro-scale roughness, such as fine soil aggregates and the surface texture of individual structural elements (e.g. Tortuosity index). However, the key advantages of the presented device are its ease of use in field conditions, ability to operate in daylight, and, most importantly, the provision of immediate roughness parameter data—eliminating the need for the extensive data processing and photogrammetric computations typically required by other methods Table 3.

Currently, the instrument calculates angles based on positional data, which, while accurate, could be further optimized. The laser ranging sensor (DEN-10–500) serves as the primary component of this instrument, constituting the predominant portion (>80 %) of the total device cost. In scenarios where reduced requirements exist for both ranging precision (e.g., ±3 mm tolerance) and measurement sampling rate (e.g., ≤100 Hz), the implementation of an economical-grade sensor variant becomes technically feasible. This configuration optimization demonstrates potential for achieving 20% cost reduction in instrumentation development while maintaining baseline functional performance. A potential improvement involves integrating an angle sensor to automatically measure the

Table 3
Comparative table between the new device and traditional methods.

Item	The method proposed by this paper	Pin meter	SfM photogrammetry	Stereo-based photogrammetry	3D Laser scanner
Cost	Medium	Low	Medium	High	High
Accuracy	Medium	Medium	Medium/High	High	High
Applicability	General, Non-contact, Bare soil	Contact, except sandy soil	Affected by ambient light and Texture information	Affected by ambient light and Texture information	Non-contact, Complex data processing
Speed	Obtain results on-site	Post processing is required	Post processing is required	Post processing is required	Post processing is required

current angle, thereby enhancing measurement speed and reducing computational overhead. While the current design demonstrates robust performance, additional protective measures could be implemented to enhance its durability during field deployment and transportation. Furthermore, to improve usability and visualization for large-scale experiments, future iterations could incorporate advanced web-based features, such as automatic GPS data integration and real-time image capture of measurement sites. These enhancements would further streamline operation and expand the instrument's applicability in diverse field settings.

CRediT authorship contribution statement

Gang Sun: Writing – review & editing, Writing – original draft, Software. **Xiu Wang:** Resources, Project administration. **Shuai Gao:** Methodology, Data curation. **Jinmei Pan:** Validation. **Qinhuo Liu:** Resources. **Wenjiang Huang:** Funding acquisition.

Declaration of competing interest

The authors declare that they have no known competing financial interests or personal relationships that could have appeared to influence the work reported in this paper.

Acknowledgments

This work was supported by the National Natural Science Foundation of China [grant numbers 42471369, 42171377]. Technical assistance for this project was provided by Xirong Yang.

References

[1] V.A. Walker, M.H. Cosh, W.A. White, A. Colliander, V.R. Kelly, P. Siqueira, Soil Surface Roughness in Temperate Forest During SMAPVEX19-22, IEEE J. Sel. Top. Appl. Earth Obs. Remote Sens. 18 (2025) 4640–4647, https://doi.org/10.1109/JSTARS.2025.3530710.
[2] K. Herodowicz-Mleczak, J. Piekarczyk, C. Kaźmierowski, J. Nowosad, M. Mleczak, Estimating Soil Surface Roughness With Models Based on the Information About Tillage Practises and Soil Parameters, J. Adv. Model. Earth Syst. 14 (2022) e2021MS002578, https://doi.org/10.1029/2021MS002578.
[3] Y. Ding, H. Geistlinger, Impact of Surface Roughness on Evaporation in 2D Micromodels, Water Resour. Res. 57 (2021) e2021WR029861, https://doi.org/10.1029/2021WR029861.
[4] L. Scalco, L. Tonietto, R.Q. Velloso, G. Racolte, L. Gonzaga, M.R. Veronez, Determination of roughness coefficient in 3D digital representations of rocks, Sci Rep 12 (2022) 10822, https://doi.org/10.1038/s41598-022-15030-y.
[5] L.M. Thomsen, J.E.M. Baartman, R.J. Barneveld, T. Starkloff, J. Stolte, Soil surface roughness: comparing old and new measuring methods and application in a soil erosion model, SOIL 1 (2015) 399–410, https://doi.org/10.5194/soil-1-399-2015.
[6] M.E. Barber, F.M. Grings, J. Álvarez-Mozos, M. Piscitelli, P.A. Perna, H. Karszenbaum, Effects of Spatial Sampling Interval on Roughness Parameters and Microwave Backscatter over Agricultural Soil Surfaces, Remote Sens. (Basel) 8 (2016) 458, https://doi.org/10.3390/rs8060458.
[7] L.L. Bourgeau-Chavez, E.S. Kasischke, K. Riordan, S. Brunzell, M. Nolan, E. Hyer, J. Slawski, M. Medvecz, T. Walters, S. Ames, Remote monitoring of spatial and temporal surface soil moisture in fire disturbed boreal forest ecosystems with ERS SAR imagery, Int. J. Remote Sens. 28 (2007) 2133–2162, https://doi.org/10.1080/01431160600976061.
[8] A.K. Fung, Z. Li, K.S. Chen, Backscattering from a randomly rough dielectric surface, IEEE Trans. Geosci. Remote Sens. 30 (1992) 356–369, https://doi.org/10.1109/36.134085.
[9] W. Jester, A. Klik, Soil surface roughness measurement—methods, applicability, and surface representation, Catena 64 (2005) 174–192, https://doi.org/10.1016/j.catena.2005.08.005.
[10] R. Bryant, M. Moran, D. Thoma, C. Collins, S. Skirvin, M. Rahman, K. Slocum, P. Starks, D. Bosch, M. Dugo, Measuring surface roughness height to parameterize radar backscatter models for retrieval of surface soil moisture, IEEE Geosci. Remote Sens. Lett. 4 (2007) 137–141, https://doi.org/10.1109/LGRS.2006.887146.
[11] Y. Oh, J.-Y. Hong, Effect of surface profile length on the backscattering coefficients of bare surfaces, IEEE Trans. Geosci. Remote Sens. 45 (2007) 632–638, https://doi.org/10.1109/TGRS.2006.888137.
[12] M. Jang, K.-J.C. Tien, J. Casanova, J. Judge, Measurements of soil surface roughness during the fourth microwave water and energy balance experiment: April 18 through June 13, 2005, Center Remote Sens., Univ. Florida, Gainesville, FL, USA, Tech. Rep (2005).
[13] A. Saleh, Soil roughness measurement: Chain method, J. Soil Water Conserv. 48 (1993) 527–529.
[14] B.B. Barreto, E. Ribeiro, F.P. Rivera, R.A.B. Junior, B. Cândido, B. McKenzie, Optical and portable equipment for characterizing soil roughness, Smart Agric. Technol. 3 (2023) 100062, https://doi.org/10.1016/j.atech.2022.100062.
[15] J. Alvarez-Mozos, N.E.C. Verhoest, A. Larrañaga, J. Casalí, M. González-Audícana, Influence of Surface Roughness Spatial Variability and Temporal Dynamics on the Retrieval of Soil Moisture from SAR Observations, Sensors (basel) 9 (2009) 463–489, https://doi.org/10.3390/s90100463.

[16] L.M. Thomsen, J.E.M. Baartman, R.J. Barneveld, T. Starkloff, J. Stolte, Soil surface roughness: comparing old and new measuring methods and application in a soil erosion model, Soil (2015) 399–410, https://doi.org/10.5194/soil-1-399-2015.
[17] A. Azizi, Y. Abbaspour-Gilandeh, T. Mesri-Gundoshmian, A.A. Farooque, H. Afzaal, Estimation of Soil Surface Roughness Using Stereo Vision Approach, Sensors 21 (2021) 4386, https://doi.org/10.3390/s21134386.
[18] Z. Alijani, J. Meloche, A. McLaren, J. Lindsay, A. Roy, A. Berg, A comparison of three surface roughness characterization techniques: photogrammetry, pin profiler, and smartphone-based LiDAR, accessed January 5, 2025, Int. J. Digital Earth (2022), https://www.tandfonline.com/doi/abs/10.1080/17538947.2022.2160842.
[19] B. Snapir, S. Hobbs, T.W. Waine, Roughness measurements over an agricultural soil surface with Structure from Motion, ISPRS J. Photogramm. Remote Sens. 96 (2014) 210–223, https://doi.org/10.1016/j.isprsjprs.2014.07.010.
[20] T. He, Y. Yang, Y. Shi, X. Liang, S. Fu, G. Xie, B. Liu, Y. Liu, Quantifying spatial distribution of interrill and rill erosion in a loess at different slopes using structure from motion (SfM) photogrammetry, Int. Soil Water Conserv. Res. 10 (2022) 393–406, https://doi.org/10.1016/j.iswcr.2022.01.001.
[21] M.W.J. Davidson, T.L. Toan, F. Mattia, G. Satalino, T. Manninen, M. Borgeaud, On the characterization of agricultural soil roughness for radar remote sensing studies, IEEE Trans. Geosci. Remote Sens. 38 (2000) 630–640, https://doi.org/10.1109/36.841993.
[22] Machine vision for soil roughness measurement and control of tillage machines during seedbed preparation, Soil Till. Res., 196 (2020) 104351. https://doi.org/10.1016/j.still.2019.104351.
[23] K.D. Mankoff, T.A. Russo, The Kinect: a low-cost, high-resolution, short-range 3D camera, Earth Surf. Proc. Land. 38 (2013) 926–936, https://doi.org/10.1002/esp.3332.
[24] S.D. Merrill, C. Huang, T.M. Zobeck, D.L. Tanaka, Use of the Chain Set for Scale-Sensitive and Erosion-Relevant Measurement of Soil Surface Roughness, D.E. Stott, R.H. Mohtar and G.C. Steinhardt (Eds). 2001. Sustaining the Global Farm. Selected Papers from the 10th International Soil Conservation Organization Meeting Held May 24-29, 1999 at Purdue University and the USDA-ARS National Soil Erosion Resear (2001) 585–591.
[25] Xu. Zhen, L. Shu, J. Wang, WATER: Dataset of surface roughness measurements in the Huazhaizi desert steppe foci experimental area, National Tibetan Plateau Data Center (2013), https://doi.org/10.3972/water973.0184.db.



Gang Sun received the M.S. and Ph.D. degrees in agricultural engineering from China Agricultural University, Beijing, China, in 2004 and 2013, respectively. He is an engineer in agricultural remote sensing study with the Aerospace Information Research Institute, Chinese Academy of Sciences, Beijing. His expertise is in the fields of remote sensing related to the agriculture.



Shuai Gao received the Ph.D. degree in remote sensing from the Institute of Remote Sensing and Applications (IRSA), Chinese Academy of Sciences, Beijing, China, in 2011. He is a research scientist with the Aerospace Information Research Institute, Chinese Academy of Sciences, Beijing. His research was focused on photogrammetry and remote sensing, including 3D reconstruction based on structure from motion (SfM) method based on the images mostly from unmanned aerial vehicle (UAV), ground truth data extraction based on LiDAR, and satellite image processing and parameters estimation using hyperspectral and multispectral satellite images, such as MODIS, Landsat, and Sentinel.



Xiu Wang received the Ph.D. degree in mechanical engineering from the China Agricultural University, Beijing, China, in 2000. He has long been engaged in the research, development, and testing of precision agricultural intelligent equipment technology. In recent years, his research has focused on automatic irrigation, precision fertilization in protected agricultural production, and efficient spraying of chemical pesticides.



Jinmei Pan graduated from The Ohio State University in 2017 with a Ph.D. She joined the State Key Laboratory of Remote Sensing Science, Aerospace Information Research Institute, Chinese Academy of Sciences, in November 2017. Her current main work includes passive microwave snow water equivalent inversion, snowmelt calculation, and snow ground measurement.



Qinhuo Liu received the Ph.D. degree from Peking University, Beijing, in 1997. He is a professor and doctoral supervisor of the Aerospace Information Research Institute, Chinese Academy of Sciences. His main research direction is the remote sensing radiative transfer mechanism and quantitative remote sensing inversion.



Wenjiang Huang received the Ph.D. degree in Cartography and GIS from Beijing Normal University, Beijing, in 2005. He is a professor in remote sensing study with the Aerospace Information Research Institute, Chinese Academy of Sciences, Beijing. His expertise is in the fields of the mechanism and application of quantitative remote sensing of vegetation. He led the constructing remote sensing monitoring, forecasting, and loss assessment methods and technical systems for vegetation diseases and insect pests and proposed a remote sensing inversion model for the vertical distribution of vegetation nutrients, realizing early non-destructive diagnosis of vegetation nutrients.